

CFD Simulation of Low-Pressure Motive Fluid of Air-Air Ejektor

By fajri vidian



CFD Simulation of Low-Pressure Motive Fluid of Air-Air Ejektor

Fajri ⁸, Jan, Ezief Muhammad Fahmi, Helmy Alian

Department of Mechanical Engineering

Universitas Sriwijaya, Sumatera - Selatan, Indonesia

Abstract:

CFD software simulation is a very effective method for predicting ejector performance according to the dimensions, working conditions, and application. Ejectors are very popular as mechanical devices for increasing fluid pressure at a lower cost. This study involved a CFD simulation of an air-air ejector using a converging-diverging nozzle. The simulation was carried out at a low motive fluid pressure of 2 kPa, 4 kPa and 6 kPa, on the range of the back pressure between 100 Pa to 670 Pa. The results showed that an increase tends to produce a reduction in the entrainment ratio. The maximum entrainment ratio is produced at a motive fluid pressure of 2 kPa of 0.84 with a critical back force of 300 kPa.

Keywords: Low Pressure, Ejector, Air, Motive Fluid, The Entrainment Ratio.

I. INTRODUCTION

The use of ejector has become a popular choice for pumping fluids, especially those at risk and vulnerable to damage when using pumps or compressors. One of the advantages of this device is its convenience and ease of operation. Many studies both simulated and experimental have been carried out in the field of ejector, that drive the secondary fluids, such as gas, steam, water, and air. Typically, air is employed as the primary motive fluid, although alternatives are being taken into consideration for this purpose. Some studies that have been conducted namely water-water ejector simulation carried out by [1], vapor-vapor conducted by [2,3,4,5,6,7,8,9,10], gas-gas by [11,12,13], steam-water by [14], water-gas by [15,16], and air-gas by [17]. To supplement the existing studies, a simulation of an air-air ejector was performed in this study. Serjosaty et al [18] conducted a subsonic air ejector simulation, and the results showed that a diameter ratio of 1.63 tends to produce the lowest air entrainment. Hernidi et al [19] carried out simulations and experiments on a supersonic air ejector with a motive fluid pressure between 3-6 bar, the results showed a deviation of 10% between both analyses. Chen et al [20] conducted simulations and experiments on a supersonic air ejector with a maximum motive fluid pressure of 6 bar. The results showed that the difference in ejector performance between both analyses in the critical mode area was 12-18% and 20% in the sub-critical. Chong et al [21] conducted a supersonic air ejector simulation with a 1 MPa motive fluid, and the results presented that the highest entrainment ratio is obtained at the optimum position of NXP. Kracík et al [22] carried out simulations and experiments of air-air ejector with 400 kPa of motive fluid, both analyses showed that the static wall pressure along ejector is highly comparable.

El-Zahaby et al [23] performed simulations of subsonic and supersonic ejector with a pressure range between 1 to 20 bar of motive fluid. One of the results indicated an increase in motive fluid pressure tends to rise the flow velocity of mixed flow of the motive and the entrained. Kumar et al [24] conducted simulations and experiments of air ejector with 5.7×10^5 Pa to determine the influence of NXP on the ejector performance, and the analyses showed comparable results. Khajeh et al [25] carried out an air-air ejector simulation using CFD to determine the effect of pressure between 100 kPa to

400 kPa on motive fluid on the efficiency of the first and second laws of thermodynamics. The results presented that the maximum and minimum efficiency of the 1st and 2nd laws are 37% and 82%, respectively. Varsegova et al [26] performed simulations of a low-pressure air-air ejector of 1371.62 Pa using CFD, and the results indicated a motive fluid between 2.15 to 2.64 kg/s and a secondary fluid of 2 kg/s. Siswantam et al [27] conducted air-air ejector simulations with fluid motive pressures between 12.6656 kPa to 37.9969 kPa and nozzle type convergeant to determine the optimum value of the constant & turbulence model, namely C_u , C_{u_0} , and C_d , which indicated 0.05, 1.48, and 1.88, respectively.

The literature review showed that the simulation of low-pressure motive fluid still rare. In this study, a CFD air-air ejector simulation was carried out with a motive fluid pressure of 2 kPa, 4 kPa, and 6 kPa using convergent-divergent type nozzles to evaluate the performance.

II. METHODOLOGY

The simulation employed the Autodesk software and was carried out using constant mixing area ejector and the convergent-divergent nozzle with the dimensions shown in Figure 1. This was carried out by applying the equations of mass, momentum, energy, and turbulence conservation. Before the simulation was carried out, the reactor image was meshed first as shown in Figure 2 using the 3D model, and the boundary conditions used are shown in Table 1.

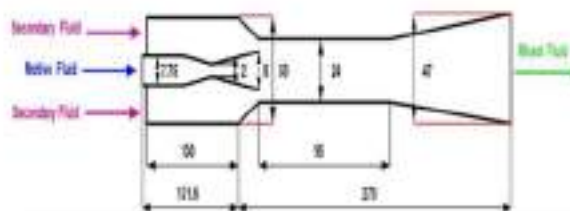




Figure 2. The meshing of ejector

Table 1. The boundary condition of the simulation

Motive Fluid Pressure (kPa(g))	Secondary Fluid Pressure (Pa(g))	Back Pressure (Pa(g))
2	0	100
		200
		300
		400
		500
		520
4	0	100
		200
		300
		400
		450
		500
6	0	600
		610
		100
		200
		300
		400
		450
		500
		550
		600
		650
		670

III. RESULTS AND DISCUSSION

Figures 3 and 4 showed an increase in flow velocity along the ejector axis. As the motive fluid pressure increased from 2 to 6 kPa, the maximum flow velocity also increased. The maximum flow velocities that occurred in the throat region of the nozzle were 47, 69, and 87 m/s for a pressure of 2, 4, and 6 kPa, respectively. These results showed a correlation with the study conducted by [23]. Then the velocity of flow in the mixing area is 31, 39, and 46 m/s for a pressure of 2, 4, and 6 kPa, respectively.

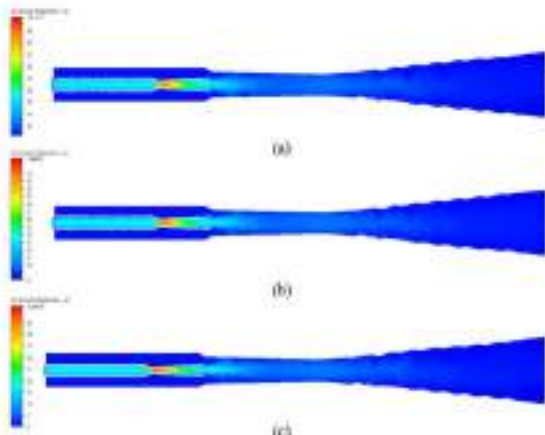


Figure 3. Flow velocity contours inside ejector: (a) 6 kPa, (b) 4 kPa, (c) 2 kPa

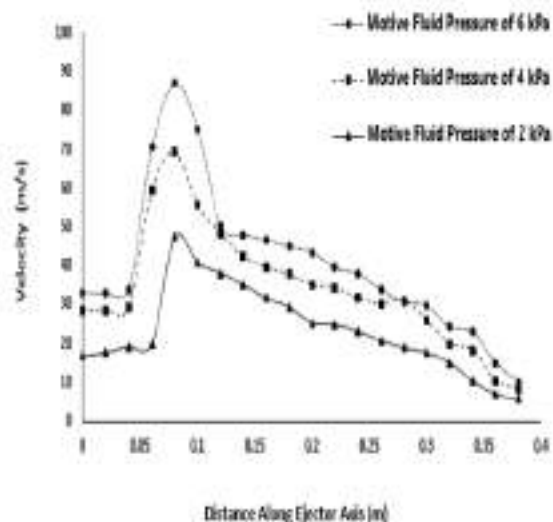


Figure 4. Flow velocity distribution along ejector axis

Figure 5 shows the contours of the static pressure dispersion inside the ejector at a motive fluid pressure of 6 kPa and a back pressure of 100 Pa. It is observed that at the exit of the nozzle, there is a vacuum area between the length of 0.1 m to 0.15 m, causing the secondary fluid to be attracted to the mixing area. Furthermore, the influence of back pressure on the distribution of static pressure inside the ejector is shown in Figure 6. Where the dispersion of static pressure inside the ejector is greater with the higher of the back pressure. These results have the same trend as the reference journal [23,27,28]. The high pressure tends to cause the secondary and primary fluid flow to be obstructed, leading to a decrease in ejector performance.

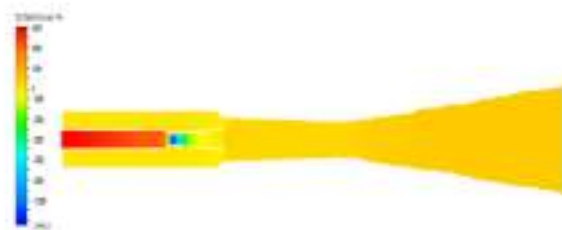


Figure 5. Static pressure distribution along ejector at 100 Pa back pressure

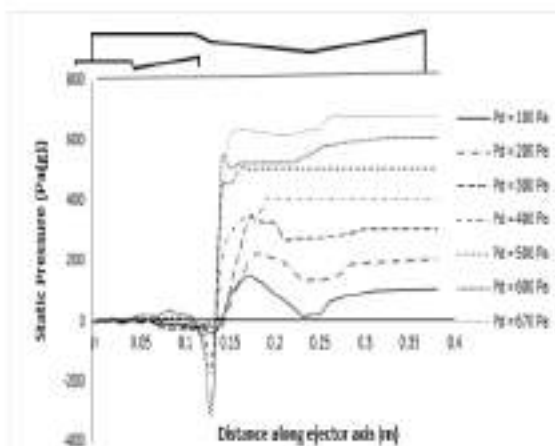


Figure 6. the distribution of static pressure of the secondary fluid along ejector at a motive fluid pressure of 600 Pa under variation of back pressure.

Figure 7 presents the highest entrainment ratio was obtained at a motive fluid pressure of 2 kPa with the value of 0.84. Above the critical back pressure of 300 Pa, the entrainment ratio tends to drop, which is in line with the study of reference [11,14]. The study indicated that at a motive fluid pressure of 4 kPa, the maximum entrainment ratio is 0.61. Then above the critical back pressure of 450 Pa, the entrainment ratio tends to drop. At a motive fluid pressure of 6 kPa, the maximum entrainment ratio tends to be 0.51. Then above the critical back pressure of 550 Pa, the entrainment ratio tends to decrease. From the simulation, it is observed that rising the motive fluid pressure tends to a drop in the entrainment ratio value and a rise in the critical back pressure. This result correlates with the simulation report of [19, 20, 27, 29].

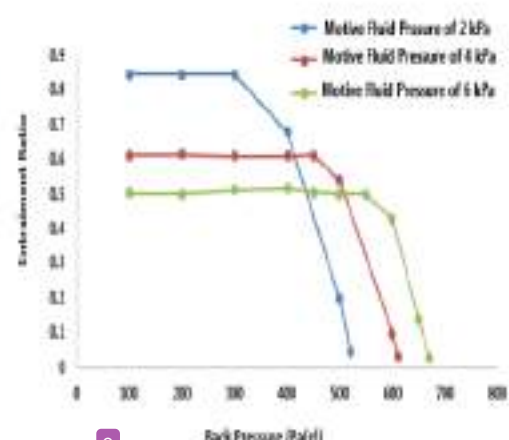


Figure 7. The influence of back pressure on the entrainment ratio

IV. CONCLUSION

The results show that a rise in motive fluid pressure from 2 kPa to 6 kPa tends to rise the distribution of flow velocity in the mixing area, and decrease the entrainment ratio. Where the entrainment ratio of 0.84, 0.61, and 0.51 was obtained from the motive fluid pressure of 2, 4 and 6 kPa, respectively. The back pressure tends to cause a drop in the entrainment ratio for each motive fluid pressure, which begins to occur after the critical phase. The critical back pressure obtained for each motive fluid pressure is 300 Pa, 450 Pa, and 550 Pa, respectively. Therefore, an increase in back pressure tends to rise the distribution pressure of the secondary fluid inside ejector.

V. REFERENCES

- [1] Marum, V.J.O., Reis, L.B., Maffei, F.S., Ranjbarzadeh, S., Koskischko, I., Gloria, R.S., Meneghini, J.R., (2021). Performance analysis of a water ejector using Computational Fluid Dynamics (CFD) simulations and mathematical modelling. Energy, 220 (119779); 1-9.
- [2] Bumrunghaichaichan, E., Ruangtrakoon, N., Thongtip, T., (2022). Performance investigation for CRMC and CPM ejectors applied in refrigeration under equivalent ejector geometry by CFD simulation. Energy Reports, 8; 12598-12617.
- [3] Al-Masae, A., Saleh, K., (2022). Supersonic Steam Ejector: Comparison of Dry and Wet- Steam CFD Simulation Models. Journal of Engineering Science and Technology, 17(2); 1200 – 1212.
- [4] Hadj, A., Boulknouar, M., (2021). CFD Analysis of Operating Condition Effects on Optimum Nozzle Exit Position of a Supersonic Ejector using The Refrigerant R134a. Comptes Rendus Mécanique, 349(1); 189-202.
- [5] Elbaraghithi, A.F.A., Mohamed, S., Nguyen, V.V., Dvorak, V., (2020). CFD Based Design for Ejector Cooling System Using HPOS (1234ze(E) and 1234yf). Energies, 13(1408); 1-19.
- [6] Riaz, F., Yam, F. Z., Qyyum, M.A., Shahzad, M.W., Farooq, M., Lee, P.S., Lee, M., (2021). Direct Analytical

- Modeling for Optimal, On-Design Performance of Ejector for Simulating Heat-Driven Systems. *Energies*, 14(2819);1-21.
- [7]. Hadi, M., Arshad, A., Shaik, N.B., Benjapolakul,W., Gillani, Q.F., (2022). Optimization Of Hydrocarbon Ejector Using Computational Fluid Dynamics, *Engineering Journal*, 26(5); 1-11.
- [8]. Zheng, J., Hou, Y., Tian, Z., Jiang, H., Chen, W., (2022). Simulation Analysis of Ejector Optimization for High Mass Entrainment under the Influence of Multiple Structural Parameters, *Energies*, 15(7058); 1-13.
- [9]. Ghonim, T.A., Hegazy, A.S., Farag, M.S., (2021). Optimization of Steam Ejector Performance Using CFD, *ERJ, PART 2, Mech. Power Eng.*, 44(3); 273 – 284.
- [10]. Suvarnakuta, N., Pianthong,K., Srivereakul, T., Seehanum, W.,(2020). Performance Analysis of a Two-Stage Ejector in An Ejector Refrigeration System using Computational Fluid Dynamics, *Engineering Application of Computational Fluid Mechanics*, 14(1); 669-682.
- [11]. Amin, A.H., Elbadawy, I., Elgendi, E., Fatouh,M., (2019),Effect of Geometrical Factors Interactions on Design Optimization Process of a Natural Gas Ejector, *Advances in Mechanical Engineering*, 11(9); 1–15.
- [12]. Setyono,A.E., Utomo, M.S.K.T.S., Aminata, J., (2022). Numerical Analysis of Geometry Ejector for Boosting Low Pressure Natural Gas, *International Journal of Engineering Research & Technology (IJERT)*, 11(06); 266-269.
- [13]. Chen, W (B), Chong, D.T., Yan, J.J., Liu, J.P., (2013). The Numerical Analysis of The Effect of Geometrical Factors on Natural Gas Ejector Performance, *Applied Thermal Engineering*, 59; 21-29.
- [14]. Han, Yu., , Wang, X., Li, A., Elburghthi, A.F.A., Wen, C.,(2022). Optimum Efficiency of a Steam Ejector for Fire Suppression Based on the Variable Mixing Section Diameter, *Entropy*, 24(1625.2022); 1-12.
- [15]. Xu, E., Jiang, X., Ding, L., Optimizing conical nozzle of venturi ejector in ejector loop reactor using computational fluid dynamics, *Korean J. Chem. Eng.*
- [16]. Utomo, T., Jin, Z., Rahman, M., Jeong, H., Chung, H.,(2008). Investigation on Hydrodynamics and Mass Transfer Characteristics of a Gas-Liquid Ejector using Three-Dimensional CFD Modelling, *Journal of Mechanical Science and Technology*, 22, 1821-1829.
- [17]. Danandono, D., Kim, K., Lee, S., Lee, J., (2011). Optimization The Design of Venturi Gas Mixer for Syngas Engine using Three-Dimensional CFD Modelling, *Journal of Mechanical Science and Technology*, 25 (9); 2285-2296.
- [18]. Surjosatyo, A., Ani, F.A., (2001). A Numerical Study of Air Flow in a Coaxial, *Jurnal Teknologi*, 34(A);1-15.
- [19]. Hemidi, A., Henry, F., Leclaire, S., Seynhaeve, J., Bartosiewicz, Y., (2009). CFD Analysis of a Supersonic Air Ejector. Part I: Experimental Validation of Single-Phase and Two-Phase Operation, *Applied Thermal Engineering*, 29; 1523-1531
- [20]. Chen, W., Liu, M., Chong, D.T., Yan, J., Blair Little,A.B., Bartosiewicz, Y., (2013). A 1D Model to Predict Ejector Performance at Critical and Sub-Critical Operational Regimes, *International Journal of Refrigeration*, 36(6):1750-1761.
- [21]. Chong, D., Hu, M., Chen, W., Wang, J., Liu, J., Yan, J., (2014). Experimental and numerical analysis of supersonic air ejector, *Applied Energy*, 130; 679–684.
- [22]. Kracik, J., Dvorak, V., (2015). Experimental and Numerical Investigation of An Air-to-Air Supersonic Ejector for Propulsion of a Small Supersonic Wind Tunnel, *EPJ Web of Conferences* 02038.
- [23]. El-Zahaby, A.M., Hamed, M.H., Orman, Z.M., Eldesokey, A.M., (2017). Study of The Configuration and Performance of Air-Air Ejectors based on CFD Simulation, *J Aeronaut Aerospace Eng.* 6 (4); 2-9.
- [24]. Kumar, V., Subbarao, P. M. V., Singhal, G., (2019). Efect of Nozzle Exit Position (NXP) on Variable Area Mixing Ejector, *SN Applied Sciences*, 1(1473); 1-9.
- [25]. Khajeh, K., Sadeghi, G., Rousholahi, R., (2020). Experimental and Numerical Thermofluidic Assessments of An Air-based Ejector Regarding Energy and Exergy Analyses, *International Communications in Heat and Mass Transfer*, 116 (104681); 1-10.
- [26]. Varsegova, E., Osipova, L., Bugembe, D.,(2021). A Study of Flow Characteristics in A Low-Pressure Ejector Installation, *E3S Web of Conferences*, 274 (08006); 1-11.
- [27]. Siswantara, A.I., Pujowidodo, H., Budiyanto, M. A., Gunadi, G.G.R., Widiauwity, C.D., (2021). An Investigation Turbulence Model of Standard k-ε to get Optimum Parameters of Turbulence Constants (c_1 , c_{21} and c_{22}) of Compressible Fluid Dynamics in a Confined Jet, *Journal of Southwest Jiaotong University*, 56 (5); 294-317.
- [28]. He, W., Wu, Y., Ma, C., (2011). Research on Ejection Coefficient of Air-Air Ejector, *IEEE*, 821-824.
- [29]. Jeong, H., Utomo, T., Ji, M., Lee, Y., Lee, G., Chung, H., (2009). CFD Analysis of Flow Phenomena inside Thermo Vapor Compressor Influenced by Operating Conditions and Converging Duct Angles, *Journal of Mechanical Science and Technology*, 23; 2366-2375.

CFD Simulation of Low-Pressure Motive Fluid of Air-Air Ejektor

ORIGINALITY REPORT

10%

SIMILARITY INDEX

PRIMARY SOURCES

- | | | |
|---|---|---------------|
| 1 | www.researchgate.net
Internet | 40 words — 2% |
| 2 | eprints.usq.edu.au
Internet | 26 words — 2% |
| 3 | www.ijert.org
Internet | 17 words — 1% |
| 4 | Sá, Diogo Nunes Couto e. "Development of a Variable Geometry Ejector for a Solar Desalination System", Universidade do Porto (Portugal), 2022
ProQuest | 14 words — 1% |
| 5 | ijesc.org
Internet | 12 words — 1% |
| 6 | savoirs.usherbrooke.ca
Internet | 11 words — 1% |
| 7 | research.usq.edu.au
Internet | 10 words — 1% |
| 8 | media.neliti.com
Internet | 9 words — 1% |
| 9 | www.mdpi.com | |

Internet

9 words — 1%

-
- 10 Yingying Tan, Youming Chen, Lin Wang. "Thermodynamic Analysis of a Mixed Refrigerant Ejector Refrigeration Cycle Operating with Two Vapor-liquid Separators", Journal of Thermal Science, 2018

Crossref

8 words — < 1%

-
- 11 kutuphane.gumushane.edu.tr

Internet

8 words — < 1%

-
- 12 Victor Jorge de Oliveira Marum. "Efficiency analysis of an incompressible-flow ejector using Computational Fluid Dynamics (CFD) simulations and mathematical modeling.", Universidade de Sao Paulo, Agencia USP de Gestao da Informacao Academica (AGUIA), 2020

Crossref Posted Content

EXCLUDE QUOTES ON
EXCLUDE BIBLIOGRAPHY ON

EXCLUDE SOURCES OFF
EXCLUDE MATCHES OFF